Journal of Materials and Environmental Sciences
ISSN : 2028-2508
CODEN : JMESCN

J. Mater. Environ. Sci., 2019, Volume 10, Issue 10, Page 926-938

http://www.jmaterenvironsci.com

Thermodynamic and DFT studies on the behavior of cefadroxil drug as effective corrosion inhibitor of copper in one molar nitric acid medium

N'guessan Yao Silvère DIKI[1]*, Nagnonta Hippolyte COULIBALY[1], Jean Simon N'Ghorand Thodhekes YAO[2, 3], Albert TROKOUREY[1]

[1]*Laboratoire de Chimie Physique, Université Félix Houphouët-Boigny, 22 BP 582 Abidjan 22, Côte d'Ivoire.*
[2]*Laboratoire de Chimie Générale, UFR Sciences Pharmaceutiques et Biologiques, Université Félix Houphouët-Boigny, 01 BP V 34, Abidjan, Côte d'Ivoire.*
[3]*Laboratoire de Nutrition, Institut National de la Santé Publique, Côte d'Ivoire.*

Received 15 April 2019,
Revised 19 Sept 2019,
Accepted 21 Sept 2019

Keywords
- ✓ *Copper,*
- ✓ cefadroxil,
- ✓ nitric acid,
- ✓ weight loss,
- ✓ Fukui functions,
- ✓ dual descriptor

dickiensil2@gmail.com

Abstract

The corrosion inhibition of copper in 1M HNO_3 solution by cefadroxil drug has been investigated in the temperature range of 298-318 K and the concentration range of 0.02-2 mM using weight loss measurement approach. The results obtained at 298 K divulged that this pharmaceutical compound had established more than 94 % inhibition efficiency at an optimum concentration of 2 mM. The adsorption of this drug on copper obeys the Langmuir isotherm. The adsorption thermodynamic functions (ΔG^{o}_{ads}, ΔH^{o}_{ads} and ΔS^{o}_{ads}) and the activation parameters (Ea, ΔH^{*}_{a}, ΔS^{*}_{a}) were determined and their values point out both physisorption and chemisorption with a predominance of physisorption. Furthermore, the quantum chemical properties/descriptors most relevant to the potential action of the compound as corrosion inhibitor such as highest occupied molecular energy (E_{HOMO}), lowest unoccupied molecular orbital energy (E_{LUMO}), energy gap (ΔE), dipole moment (μ) and charges on heteroatoms were computed using DFT at B3LYP level with 6-31G (d, p) basis set. Fukui functions and dual descriptor were also determined and discussed. The theoretical results are consistent with the experimental data to good extend

1. Introduction

Copper and its alloys are widely used in many industries and applications (industrial equipment, tubes, wires production, electricity and electronics, etc.) due to its excellent electrical and mechanical properties [1-4]. Thus, corrosion of copper and its inhibition in aggressive media has focused many researches [5-8]. Among several methods used in combating corrosion problems, the use of chemical inhibitors remains the most cost effective and practical one [9-11].

Therefore, heterocyclic compounds [12] are employed as corrosion inhibitors because the presence of many adsorption centers (O, N, S, P, and π electrons) helps them to form complexes with metal ions. These complexes constitute a film barrier which separates the metal from the aggressive environment [13].

A review of literature [14, 15] indicates that cefadroxil has been studied as a corrosion inhibitor for steel and aluminum in an acid medium. However, the inhibitive properties of this compound against copper corrosion are reported for the first time through this paper. Cefadroxil is the commercial name of 7β - {[(2r) -2-amino-2- (4-hydroxyphenyl) acetyl] amino} -2, 3-didehydrocepham-2-carboxylic acid having molecular formula of $C_{16}H_{17}N_3O_5S$ and 363.389 $gmol^{-1}$ as molecular mass.

The aim of the present paper is to establish the relationship between the calculated quantum chemical parameters and the experimentally determined inhibition efficiency of cefadroxil drug (Scheme 1) against copper corrosion in one molar nitric acid medium. This can be achieved by computing the most relevant electronic properties of the studied drug including global parameters such as E_{HOMO}, E_{LUMO}, energy gap (ΔE), dipole moment (μ), electronegativty (χ), global hardness (η), glogal softness(S), fraction of electrons transferred (ΔN) as well as local ones (Fukui functions and dual descriptor).

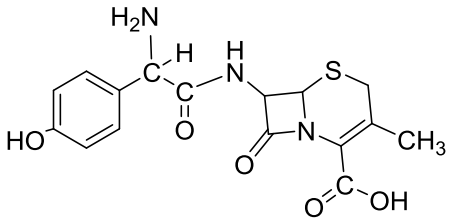

Scheme 1: Chemical structure of cefadroxil.

2. Experimental details

2.1 Copper samples

The copper specimens were in form of rod measuring 10 mm in length and 2.2 mm of diameter. They were cut in commercial copper of purity 95 %.

2.2 The studied inhibitor

It is a first-generation cephalosporin antibiotic drug that is the para-hydroxy derivative of cefalexin, and is used similarly in the treatment of mild to moderate susceptible infections such as the bacterium *Streptococcus pyogenes*, causing the disease popularly called strep throat or streptococcal tonsillitis, urinary tract infection, reproductive tract infection, and skin infections.

2.3 Solutions

Analytical grade 65 % nitric acid solution from Sigma-Aldrich Chemicals was used to prepare the corrosive aqueous solution. The solution was prepared by dilution of the commercial nitric acid solution using double distilled water. The blank was a 1M HNO_3 solution. Solutions of cefadroxil with concentrations in the range of 0.02 mM to 2 mM were prepared. Acetone of purity 99.5% was also purchased from Sigma-Aldrich Chemicals.

2.4 Weight loss technique

Prior to all measurements, the copper samples were mechanically abraded with different grade emery papers (1/0, 2/0, 3/0, 4/0, 5/0, and 6/0). The specimens were washed thoroughly with double distilled water, degreased and rinsed with acetone and dried in a moisture-free desiccator. Weight loss measurements were carried out in a beaker of 100 mL capacity containing 50 mL of the test solution. The immersion time for weight loss was 1h at a given temperature. In order to get good reproducible data, parallel triplicate experiments were performed accurately and the average weight loss was used to calculate the corrosion rate (W), the degree of surface coverage (Ɵ) and the inhibition efficiency (IE) using Equation 1-3 respectively:

$$W = \frac{m_1 - m_2}{St} \quad (1)$$

$$\theta = \frac{W_0 - W}{W_0} \quad (2)$$

$$IE(\%) = \left(\frac{W_0 - W}{W_0}\right) * 100 \quad (3)$$

where W_0 and W are the corrosion rate without and with inhibitor respectively, m_1 and m_2 are the weight before and after immersion in the corrosive aqueous solution respectively, S is the total surface of the copper specimen and t is the immersion time.

2.5 Computational details

In order to explore the theoretical-experimental consistency, quantum chemical calculations were performed using Gaussian 09 W package [16]. In the present calculations, we have used Becke's three parameter exchange functional along with the Lee-Yang-Parr non local correlation functional (B3LYP)[17] using 6-31G(d,p) basis set

Global parameters

The molecular descriptors such as the energy of the highest occupied molecular orbital (E_{HOMO}), the energy of the lowest unoccupied molecular orbital (E_{LUMO}), the energy gap ($\Delta E = E_{LUMO} - E_{HOMO}$), the dipole moment (μ) and the total energy (E) of the molecule were computed. The reactivity parameters were then calculated using the conceptual framework of DFT [18, 19]. So, the chemical potential μ_p is defined as (Equation 4):

$$\mu_p = \left(\frac{\partial E}{\partial N}\right)_{v(r)} = -\chi \quad (4)$$

where μ_p is the chemical potential, E is the total energy, N is the number of electrons, v(r) is the external potential of the system and χ is the global electronegativity. The global hardness is given by Equation 5 the equation below:

$$\eta = \left(\frac{\partial^2 E}{\partial N^2}\right)_{v(r)} \quad (5)$$

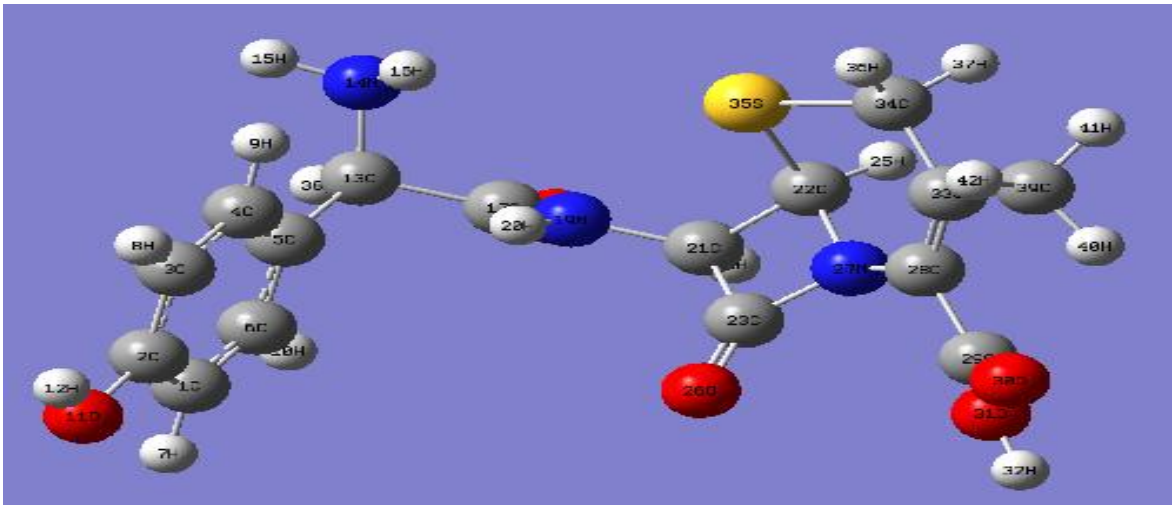

Figure 1: Optimized structure of cefadroxil calculated by B3LYP/6-31 G (d, p).

Using the finite difference approximation and the Koopmans theorem, the global electronegativity and the global hardness are given by Equation 6 and 7 respectively:

$$\chi = \frac{(I+A)}{2} \approx -\frac{(E_{HOMO}+E_{LUMO})}{2} \quad (6)$$

$$\eta = \frac{(I-A)}{2} \approx \frac{(E_{LUMO}-E_{HOMO})}{2} \quad (7)$$

The global softness which is the reciprocal of the global hardness can be obtained using Equation 8:

$$S = \frac{1}{\eta} \quad (8)$$

The ionization potential is the negative of E_{HOMO} (Equation 9)

$$I = -E_{HOMO} \quad (9)$$

The electron affinity is the negative of E_{LUMO} (Equation 10)

$$A = -E_{LUMO} \quad (10)$$

The electrophilicity index ω [20] is defined as:

$$\omega = \frac{\mu_p^2}{2\eta} \quad (11)$$

According to the definition, this index measures the propensity of chemical species to accept electrons. A high value of electrophilicity index describes a good electrophile behavior while a small value of electrophilicity index describes a good nucleophile behavior.

The fraction of electrons transferred (ΔN) is given by Equation 12 [21]:

$$\Delta N = \frac{\chi_{C_u} - \chi_{inh}}{2(\eta_{C_u} + \eta_{inh})} \quad (12)$$

The values of experimental work function $\chi_{C_u} = 4.98\ eV$ [20] and hardness $\eta_{C_u} = 0$ [22] (since for bulk metallic atoms $I = A$) were considered to calculate ΔN. This new reactivity index measures the stabilization in energy when the system acquires an additional electronic charge ΔN from the environment [23].

Local parameters

The Fukui functions were used to analyze the local reactivity of cefadroxil as a corrosion inhibitor of copper. The condensed Fukui functions and condensed local softness are parameters which enable us to distinguish each part of the studied compound on the basis of its chemical behavior due to different substituent

functional groups. The Fukui function is defined as the derivative of the electronic density ρ(r) with respect to the number N of electrons:

$$f(r) = \left(\frac{\partial \rho(r)}{\partial N}\right)_{v(r)} \quad (13)$$

The condensed Fukui functions provide information about atoms in a molecule that have a tendency to either donate (nucleophilic character) or accept (electrophilic character) an electron or a pair of electrons [24]. The nucleophilic and electrophilic Fukui function for an atom k [25] can be computed using a finite difference approximation as seen in

$$f_k^+ = [q_k\,(N+1) - q_k(N)\,] \text{ for nucleophilic attack} \quad (14)$$
$$f_k^- = [q_k\,(N) - q_k(N-1)\,] \text{ for electrophilic attack} \quad (15)$$

where $q_k\,(N+1)$, $q_k(N)$ and $q_k(N-1)$ are the charges of the atoms on the systems with (N+1), N and N-1 electrons respectively.

It has been reported recently [26] that a new descriptor has been introduced [27, 28] which allows the determination of individual sites within the molecule with particular behaviors. A mathematical analysis reveals that dual descriptor is a more accurate tool than nucleophilic and electrophilic Fukui functions [29]. This descriptor is defined as:

$$\Delta f(r) = \left(\frac{\partial f(r)}{\partial N}\right)_{v(r)} \quad (16)$$

The condensed form [27] of the dual descriptor is given as:

$$\Delta f_k(r) = f_k^+ - f_k^- \quad (17)$$

When $\Delta f_k(r) > 0$, the process is driven by a nucleophilic attack and atom k acts as an electrophile; conversely, when, $\Delta f_k(r) < 0$ the process is driven by an electrophilic attack on atom k acts as a nucleophile. The dual descriptor $\Delta f_k(r)$ is defined within the range {–1;1}, what really facilitates interpretation [29].

3. Results and discussion

3.1 Weight loss measurement

Figure 2 gives the representation of corrosion rate versus temperature for different concentrations in cefadroxil.

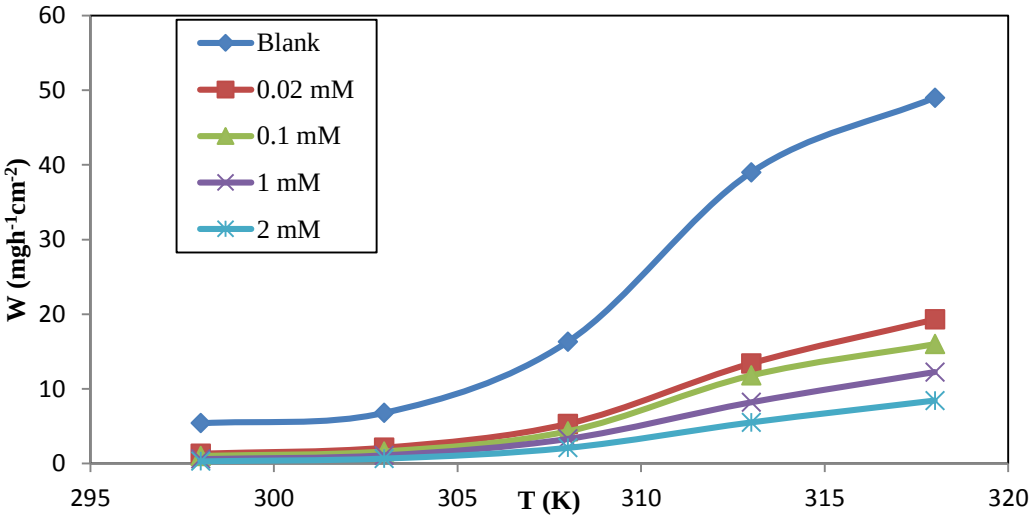

Figure 2: Evolution of corrosion rate versus temperature for different concentrations of cefadroxil.

It can be seen that over the temperature range studied, corrosion rate increases with increasing temperature. However, the rise in cefadroxil concentration affects the evolution of the corrosion rate which decreases when the concentration increases, indicating that the protection ability of the studied drug was concentration dependent. Figure 3 presents the evolution of inhibition efficiency with temperature for different concentrations.

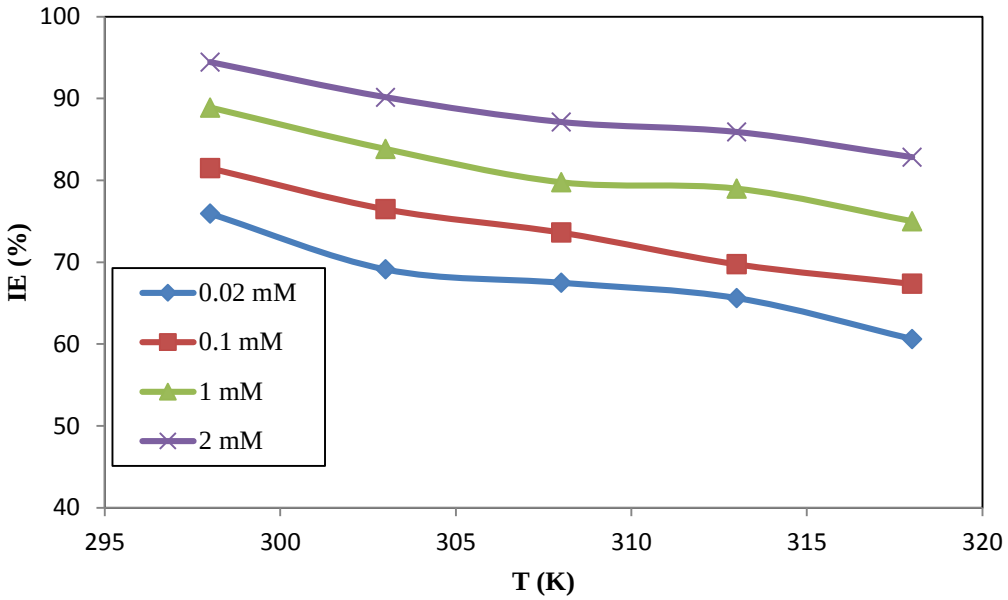

Figure 3: Inhibition efficiency versus temperature for different concentrations of cefadroxil.

Inhibition efficiency increases with increasing temperature for all the range of concentrations. For a given temperature, inhibition efficiency increases when the concentration increases. All these observations show that cefadroxil acts as an effective inhibitor of copper corrosion over the concentration range studied. This behavior could be explained by the formation of a barrier which separates copper from the nitric acid solution [13].

3.1.1 Adsorption considerations

Attempts were made to fit values of Θ to three isotherms including Langmuir, El-Awady and Flory-Huggins. The best fit was obtained with the Langmuir adsorption model whose equation is written as follows:

$$\frac{C_{inh}}{\theta} = \frac{1}{K_{ads}} + C_{inh} \qquad (18)$$

where C_{inh} is the concentration of the inhibitor and K_{ads} is the equilibrium constant in the adsorption process. A linear relationship between $\frac{C_{inh}}{\theta}$ and C_{inh} (Figure 4) has been observed with correlation coefficient near unity. The obtained Langmuir adsorption parameters for different temperatures are displayed in. Given that the correlation coefficients (R^2) and the slopes are very close to unity (Table 1), the studied inhibitor adsorbs on copper surface through Langmuir isotherm model.

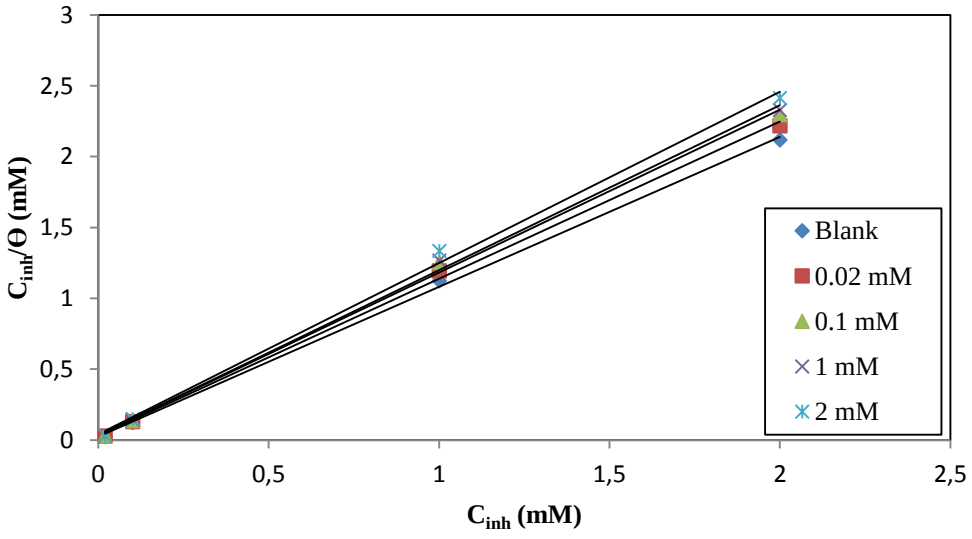

Figure 4: Langmuir adsorption isotherm for cefadroxil on copper surface in 1M HNO_3.

Table 1: Regression parameters of Langmuir isotherm.

Isotherm model	T(K)	R^2	Slope	Intercept
Langmuir	298	0.9991	1.0585	0.0223
	303	0.9986	1.1092	0.0276
	308	0.9979	1.1494	0.0322
	313	0.9981	1.1638	0.0342
	318	0.9973	1.2083	0.0400

The equilibrium constant (K_{ads}) is related to the free energy of adsorption (ΔG^0_{ads}) [30] by:

$$\Delta G^0_{ads} = -RTln(55.5K_{ads}) \quad (19)$$

In the above equation, 55.5 is concentration of water in mol L^{-1}, *T* is absolute temperature while *R* is universal gas constant. The values of ΔG^0_{ads} and other thermodynamic functions are summarized in table 2.

Table 2: Adsorption thermodynamic functions.

T (K)	K_{ads} (M^{-1})	ΔG^0_{ads} ($kJ\ mol^{-1}$)	ΔH^0_{ads} ($kJ\ mol^{-1}$)	ΔS^0_{ads} ($J\ mol^{-1}K^{-1}$)
298	44843.05	–36.47		
303	36231.88	–36.55		
308	31055.90	–36.75	–21.74	49.10
313	29239.77	–37.19		
318	25000.00	–37.37		

Negative values of ΔG^0_{ads} indicate a spontaneous adsorption process and stability of the adsorbed layer [31] on the copper surface. Literature [30, 32] state that values of ΔG^0_{ads} around –40 kJ mol^{-1} or more negative are associated with chemisorption while these of –20 kJ mol^{-1} or less negative indicate physisorption. The values displayed in Table 2 suggest both, chemisorption and physisorption. The changes in adsorption enthalpy and entropy were obtained using the following equation:

$$\Delta G^0_{ads} = \Delta H^0_{ads} - T\Delta S^0_{ads} \quad (20)$$

According to equation (20), thermodynamic adsorption parameters ΔH^0_{ads} and $(-\Delta S^0_{ads})$ can be determined respectively as the intercept and slope of the straight line obtained by plotting ΔG^0_{ads} versus temperature (Figure 5).

3.1.2 Effect of the temperature and activation parameters

Activation parameters are of great importance in the study of the inhibition mechanism of metals. The kinetics functions for the dissolution of copper without and with various concentrations of the studied inhibitor are obtained [33] by applying the Arrhenius equation and the transition state equation:

$$logW = logk - \frac{E_a}{2.303RT} \quad (21)$$

$$log\left(\frac{W}{T}\right) = [log(\frac{R}{\aleph h}) + \frac{\Delta S^*_a}{2.303R}] - \frac{\Delta H^*_a}{2.303RT} \quad (22)$$

In these equations, E_a is the activation energy, k is the Arrhenius pre-exponential factor; h is the Planck's constant, $\aleph$ is the Avogadro number, ΔS^*_a is the change in activation entropy and ΔH^*_a is the change in activation enthalpy.

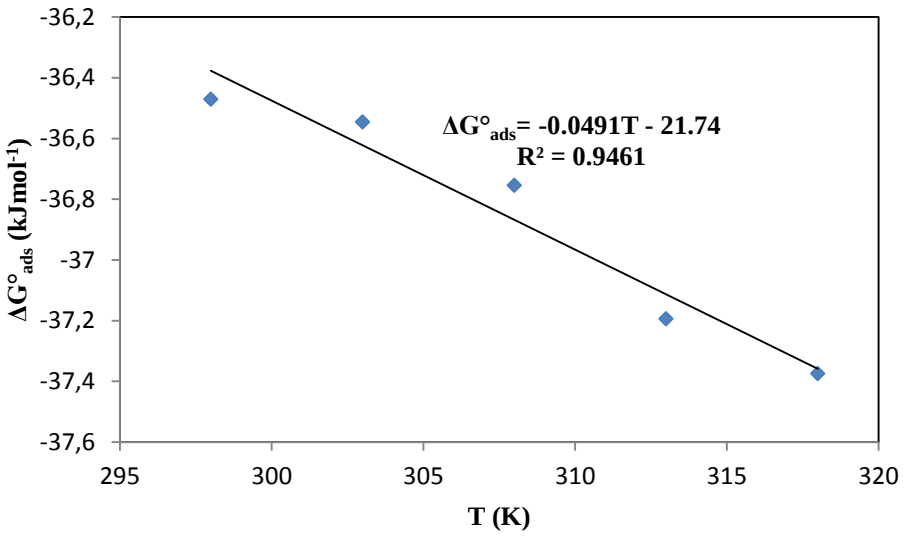

Figure 5: ΔG^{0}_{ads} versus T for the adsorption of cefadroxil on copper in 1M HNO_3.

Figure 6 and Figure 7 display respectively the plots of $logW$ and $log\left(\frac{W}{T}\right)$ versus $\frac{1}{T}$.

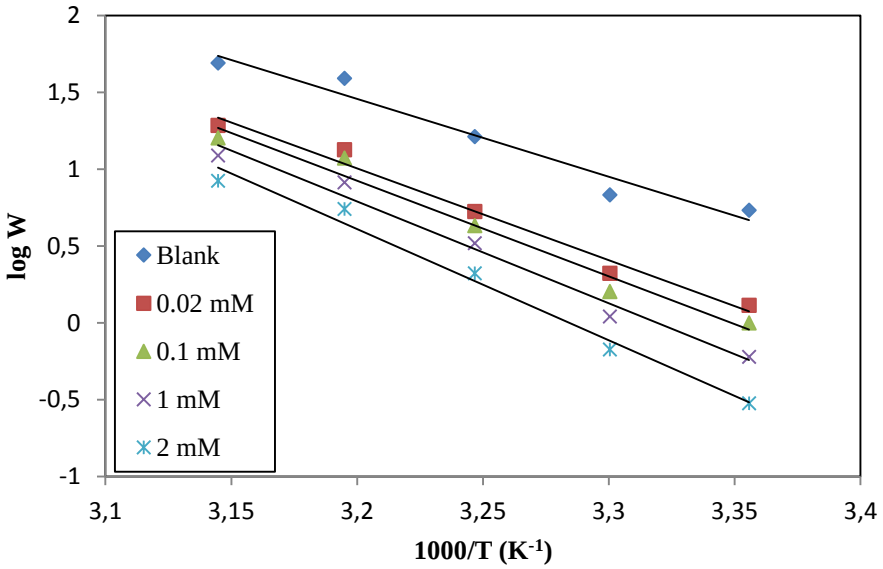

Figure 6: Arrhenius plots for copper corrosion in 1M HNO_3 solutions without or with cefadroxil.

All graphs show, both in absence and presence of the studied inhibitor excellent linearity as expected from equations (21) and (22), respectively. The intercepts of the lines in Figure 6 allow the calculation of the values of the pre-exponential factor (k) and the slopes $(-\frac{E_a}{2.303R})$ lead to the determination of the activation energy E_a both in the absence and presence of the inhibitor. The straight lines obtained by plotting $log\left(\frac{W}{T}\right)$versus $\frac{1}{T}$ (Figure 7) have $(-\frac{\Delta H_a^*}{2.303R})$ as slope and $[log(\frac{R}{\aleph h}) + \frac{\Delta S_a^*}{2.303R}]$ as intercept. Consequently, the values of ΔH_a^* and ΔS_a^* were calculated and presented in Table 3.

From Table 3, it seems that E_a and ΔH_a^* varied in the same manner increasing with the concentration, probably due to the thermodynamic relation between them $(\Delta H_a^* = E_a - RT)$. It can be seen that the values of E_a are higher in the inhibited solutions than those in uninhibited solutions. On the other hand, the higher values of E_a in the presence of inhibitor compared to that in its absence and the decrease of the inhibition efficiency (IE) with the increase in temperature can be interpreted as an indication of predominant physical adsorption process [34, 35].

Moreover, the positive signs of ΔH_a^* reflected the endothermic effect of the copper dissolution process. The value of ΔS_a^* is higher for the inhibited solution than that for the uninhibited solution. This phenomenon suggested that a randomness decrease occurred from reactants to the activated complex. This might be the result of the adsorption of organic inhibitor molecules from the acidic solution which could be regarded as a quasi-substitution process between the organic compound in the aqueous phase and water molecules at the copper surface [36].

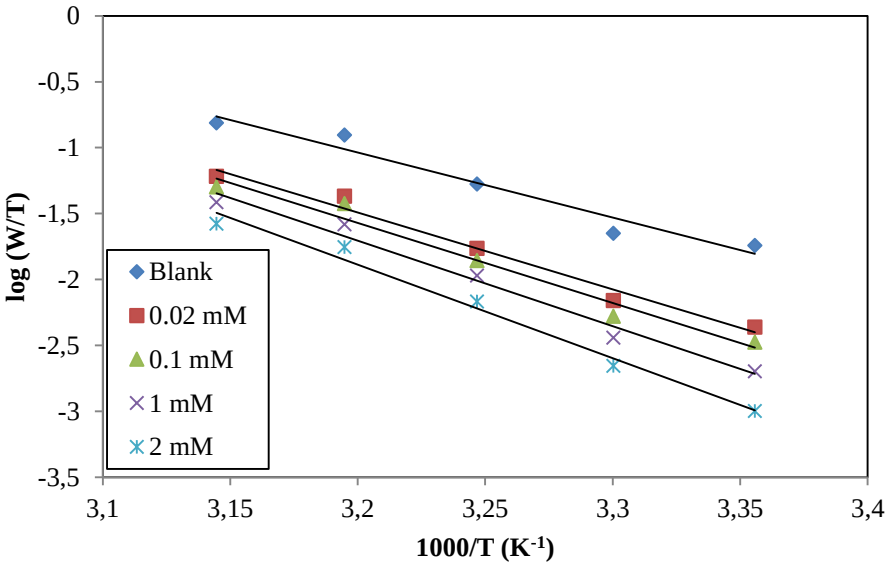

Figure 7: Transition state plots for copper corrosion in 1M HNO_3 without or with cefadroxil.

Table 3: Activation parameters for copper corrosion without or with cefadroxil in 1M HNO_3.

System	E_a (kJmol^{-1})	ΔH_a^* (kJmol^{-1})	ΔS_a^* (Jmol^{-1}K^{-1})
Blank	96.97	94.29	84.68
0.02 mM	114.23	111.52	131.16
0.1 mM	118.88	116.16	144.48
1 mM	126.80	124.08	167.23
2 mM	138.42	135.69	200.94

3.2 Quantum chemistry

3.2.1 Global reactivity

The calculated quantum chemical parameters are displayed in Table 4. According to the frontier molecular orbital theory (FMO) of chemical reactivity, transition of electron is due to interaction between highest occupied molecular orbital (HOMO) and lowest unoccupied molecular orbital (LUMO) of reacting species [37]. E_{HOMO} is a quantum chemical parameter which is often associated with the electron donating ability of the molecule. High value of E_{HOMO} is likely to a tendency of the molecule to donate electrons to appropriate acceptor molecule of low empty molecular orbital energy [38]. The inhibitor does not only donate electron to the unoccupied d orbital of the metal ion but can also accept electron from the d orbital of the metal leading to the formation of a feedback bond. The highest value of E_{HOMO} (-6.0965 eV) of cefadroxil indicates a good inhibition efficiency. The LUMO energy orbital is consistent with electron accepting ability of a molecule. Lower value of E_{LUMO} for a molecule [38] implies good electron accepting ability. The obtained value (E_{LUMO}= –1.4525 eV) is low when compared with that of some molecules in the literature [39]; so, the studied molecule could receive electrons from copper.

Table 4: Quantum chemical parameters of cefadroxil.

Descriptor	Value	Descriptor	Value
E_{HOMO} (eV)	–6.0965	I (eV)	6.0965
E_{LUMO} (eV)	–1.4525	A (eV)	1.4525
ΔE (eV)	4.6440	**μ** (Debye)	4.5054
ΔN	0.1089	Ƞ (eV)	2.3220
S $(eV)^{-1}$	0.4306	**ω**	2.0780
χ (eV)	3.7745	TE (a.u)	–1558.5177

The energy gap, ($\Delta E = E_{LUMO} - E_{HOMO}$) is an important parameter as a function of reactivity of the inhibitor molecule towards the adsorption on the metallic surface. As ΔE decreases, the reactivity of the molecule increases leading to increase in the inhibition efficiency of the molecule. Lower values of the energy difference will render good inhibition efficiency, because the energy to remove an electron from the last occupied orbital will be low [40]. In the present work, the low value of energy gap (ΔE = 4.6440 eV) could explain the high inhibition efficiency values (IE= 94.44 % for C_{inh}=2 mM at T = 298 K).

Another important electronic parameter assessed is the dipole moment (μ) that results from non-uniform distribution of charges on atoms in the molecule. Several authors state that low values of dipole moment [41] promote accumulation of the inhibitor molecules in the surface layer and therefore higher inhibition efficiency. However, many papers indicate that inhibition efficiency increases with rising values of dipole moment. On the other hand, survey of the literature [42, 43] reveals that several irregularities appeared in case of correlation of dipole moment with inhibitor efficiency. So, in general [44], there is no significant relationship between dipole moment values and inhibition efficiencies.

Global hardness and softness are important parameters to measure respectively the molecular stability and reactivity of a molecule. The chemical hardness fundamentally represents the resistance towards the deformation or polarization of the electron cloud of atoms, ions or molecules under small perturbation of chemical reaction. A hard molecule has a large energy gap and a soft molecule has a small energy gap [45]. In the present work, the studied compound has a low hardness value (2.5368 eV) and a high value of softness $(0.3942eV)^{-1}$ when compared [23, 46] with molecules in the literature.

The ionization potential (I) and the electronic affinity (A) are respectively (5.734 eV) and (0.559 eV). This low value of (I) and the high value of electron affinity indicate the capacity of the molecule both to donate and accept electron. The electronegativity (χ) indicates the capacity of a system to attract electrons. In our work, the low value of the electronegativity of the studied molecule ($\chi = 3.247eV$) when compared to that of copper ($\Phi_{Cu} =$ 4.98 eV) shows that copper has the better attraction capacity. Then the low value of hardness (2.587 eV) confirms the relatively higher value of the fraction of electrons transferred (ΔN = 0.2036) indicating a possible motion of electrons from the inhibitor to the metal. The electrophilicity index measures the propensity of chemical species to accept electrons; a high value of electrophilicity index describes a good electrophile while a small value of electrophilicity index describes a good nucleophile. In this work the obtained value (ω = 2.0780 eV) shows the good capacity of cefadroxil to accept electrons.

3.2.2 Local reactivity

The local reactivity can be analyzed through atomic charges, condensed Fukui functions and the newly introduced parameter (dual descriptor) that enable to distinguish each part of the molecule on the basis of its distinct chemical behavior due to different substituent functional groups. The Fukui function is motivated by the fact that if an electron δ is transferred to an N electron molecule, it will tend to distribute and so minimize the energy of the resulting N + δ electron system [47]. Thus nucleophilic attack will occur where f_k^+ value is maximum and $\Delta f_k(r)$ is positive whereas the electrophilic attack will occur where f_k^- is maximum and $\Delta f_k(r)$ is negative. The computed Mulliken atomic charges, Fukui functions and dual descriptor by DFT at the B3YLP/6-31G (d, p) level are displayed in Table 5.

Table 5: computed Mulliken atomic charges, Fukui functions and dual descriptor of some selected atoms of cefadroxil by DFT B3YLP 6-31/ G (d, p).

Atom	q_k *(N+1)*	q_k *(N)*	q_k *(N-1)*	f_k^+	f_k^-	Δf
1 C	-0.101	-0.095	-0.110	-0.006	0.015	-0.021
2 C	-0.320	0.330	0.354	-0.650	-0.024	-0.626
3 C	0.136	-0.129	-0.077	**0.265**	-0.052	**0.317**
4 C	-0.142	-0.151	-0.103	0.009	-0.048	0.057
5 C	0.115	0.090	0.102	0.025	-0.012	0.037
6 C	-0.124	-0.119	-0.084	-0.005	-0.035	0.030
11 O	-0.574	-0.555	-0.477	-0.019	-0.078	0.059
13 C	-0.085	-0.089	-0.078	0.004	-0.011	0.015
14 N	-0.612	-0.588	-0.636	-0.024	0.048	-0.072
17 C	0.580	0.607	0.596	-0.027	0.011	-0.038
18 O	-0.533	-0.498	-0.471	-0.035	-0.027	-0.008
19 N	-0.465	-0.518	-0.506	0.053	-0.012	0.065
21 C	-0.075	-0.043	-0.051	-0.032	0.008	-0.040
22 C	-0.030	-0.073	-0.086	0.043	0.013	0.030
23 C	0.595	0.575	0.599	0.020	-0.024	0.044
26 O	-0.484	-0.452	-0.395	-0.032	-0.057	0.025
27 N	-0.503	-0.512	-0.489	0.009	-0.023	0.032
28 C	0.205	0.243	0.256	-0.038	-0.013	-0.025
29 C	0.530	0.553	0.554	-0.023	-0.001	-0.022
30 O	-0.484	-0.477	-0.426	-0.007	-0.051	0.044
31 O	-0.523	-0.473	-0.476	-0.050	0.003	-0.053
33 C	0.153	0.085	0.093	0.068	-0.008	0.076
34 C	-0.273	-0.406	-0.423	0.133	0.017	0.116
35 S	-0.515	0.110	0.174	-0.625	-0.064	-0.561
39 C	-0.360	0.085	-0.362	-0.445	**0.447**	**-0.892**

It can be seen from shaded raws in Table 5 that (3 C) with the maximum value of f_k^+ and positive value of $\Delta f_k(r)$ is the most probable nucleophilic attack site, while (39 C) with the maximum value of f_k^- and negative value of $\Delta f_k(r)$ is the most probable electrophilic attack site. These sites are indicated by the arrows on the HOMO and LUMO densities (Figure 8).

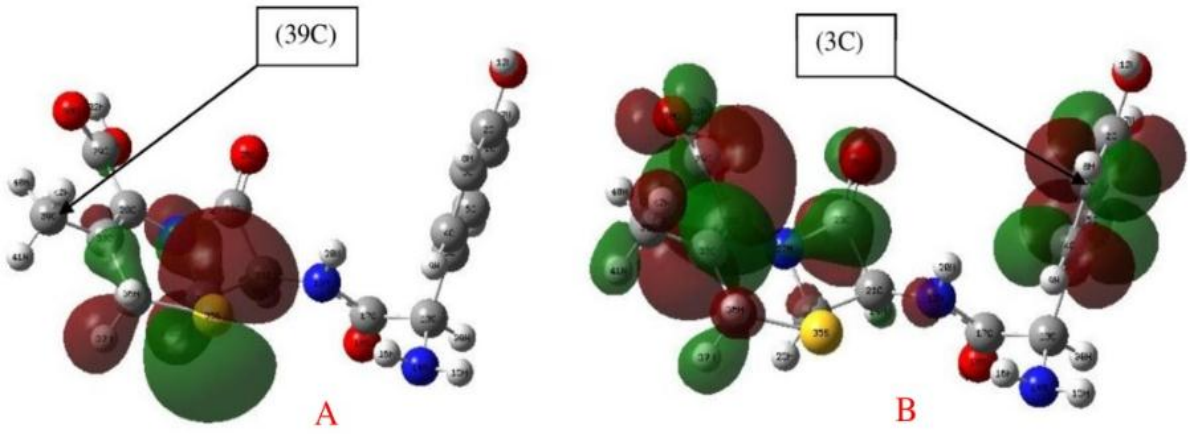

Figure 8: HOMO (A) and LUMO (B) densities calculated by B3LYP/6-31G (d, p).

Conclusion

From the results of the present study, cefadroxil is a good inhibitor for the corrosion of copper in one molar nitric acid medium. The inhibition efficiency of this drug is concentration and temperature dependant. The adsorption of cefadroxil on copper surface is spontaneous and obeys the mechanism of physical as well as chemical adsorption from the calculated thermodynamic data. The experimental data obtained in the study fitted the Langmuir adsorption isotherm (mean $R^2 = 0.9982$) best. Quantum chemical calculations using the DFT B3LYP/6-31G (d, p) level revealed that the sites for nucleophillic and electrophillic attacks are carbon (3 C) and carbon (39 C) respectively.

References

1. X. Zhang, W. He, I. O. Wallinger, J. Pan, and C. Leygraf, Determination of instantaneous corrosion rates and runoff rates of copper from naturally patinated copper during continuous rain events, *Corros. Sci.,* 44 (2002) 2131-2151
2. X. Zhang, W. He, I. O. Wallinger, and C. Leygraf, Mechanistic studies of corrosion product flaking on copper and copper-based alloys in marine environments, *Corros. Sci.,* 85 (2014) 15-25
3. E. Szöcs, G. Vestag, A. Shaban, G. Kouczos, and E. Kalman, Investigation of copper corrosion inhibition by STM and EQCM techniques, *J. Appl. Electrochem.,* 29 (1999) 1339-1345
4. M. Vincent, P. Hartemann, and M. Engels-Deutsch, Antimicrobial applications of copper, *Int. J. Hyg. Environ. Health.,* 219 (2016) 585-591
5. H. S. Gadow, T. A. Farghaly, and A. M. Eldesoky, Experimental and theoretical investigations for some spiropyrazoles derivatives as corrosion inhibitors for copper in 2 M HNO3 solutions, *J. Mol. Liq.,* 294 (2019) 111614-111634
6. L. H. Madkour, S. Kaya, and I. B. Obot, Computational, Monte Carlo simulation and experimental studies of some arylazotriazoles (AATR) and their copper complexes in corrosion inhibition process, *J. Mol. Liq.,* 260 (2018) 351-374
7. A. Zarrouk, B. Hammouti, A. Dafali, M. Bouachrine, H. Zarrok, S. Boukhris, *et al.,* A theoretical study on the inhibition efficiencies of some quinoxalines as corrosion inhibitors of copper in nitric acid, *J. Saudi Chem. Soc.,* 18 (2014) 450-455
8. G. Karthik and M. Sundaravadivelu, Investigations of the inhibition of copper corrosion in nitric acid solutions by levetiracetam drug, *Egypt. J. Pet.,* 25 (2016) 481-493
9. V. Kouakou, P. M. Niamien, A. J. Yapo, S. Diaby, and A. Trokourey, Experimental and DFT Studies on the Behavior of Caffeine as Effective Corrosion Inhibitor of Copper in 1M HNO_3, *Orbital: Electron. J. Chem.,* 8 (2016) 66-79
10. A. D. Ehouman, G. G. D. Diomandé, P. M. Niamien, D. Sissouma, and A. Trokourey, 2-Thiobenzyl-6-methylbenzoxazole as an effective copper corrosion inhibitor in 2M HNO3: experimental and DFT studies, *IOSR J. Appl. Chem.,* 9 (2016) 17-25
11. M. A. Tigori, P. M. Niamien, A. J. Yapo, and A. Trokourey, Effect of pyridoxine hydrochloride on copper corrosion in 1M HNO3, *J. Chem. Biol. Phys. Sci.,* 6 (2016) 1201-1216
12. S. L. Cohen, V. A. Brusic, F. B. Kaufman, G. S. Frankel, S. Motakef, and B. Rush, Xray photoelectron spectroscopy and ellipsometry studies of the electrochemically controlled adsorption of benzotriazole on copper surfaces, *J. Vac. Sci. Technol. A.,* 8 (1990) 2417-2424
13. N. Y. S. Diki, G. K. Gbassi, A. Ouedraogo, M. Berte, and A. Trokourey, Aluminum corrosion inhibition by cefixime drug: experimental and DFT studies, *J. Electrochem. Sci. Eng.,* 8 (2018) 303-320
14. N. Y. S. DIKI, K. V. BOHOUSSOU, M. G.-R. KONE, A. OUEDRAOGO, and A. TROKOUREY, Cefadroxil Drug as Corrosion Inhibitor for Aluminum in 1 M HCl Medium: Experimental and Theoretical Studies, *IOSR J. Appl. Chem.,* 11 (2018) 24-36
15. S. K. Shukla, M. A. Quraishi, and E. E. Ebenso, Adsorption and corrosion inhibition properties of cefadroxil on mild steel in hydrochloric acid, *Int. J. Electrochem. Sci.,* 6 (2011) 2912-2931
16. M. J. Frisch, G. W. Trucks, G. E. S. H. B. Schlegel, M. A. Robb, J. R. Cheeseman, G. Scalmani, V. Barone, B. Mennucci, G. A. Petersson, H. Nakatsuji, M. Caricato, X. Li, H. P. Hratchian, A. F. Izmaylov, J. Bloino, G. Zheng, J. L. Sonnenberg, M. Hada, M. Ehara, K. Toyota, R. Fukuda, J. Hasegawa, M. Ishida, T. Nakajima, Y. Honda, O. Kitao, H. Nakai, T. Vreven, J. A. Montgomery, Jr., J. E. Peralta, F. Ogliaro, M. Bearpark, J. J. Heyd, E. Brothers, , and V. N. S. K. N. Kudin, R. Kobayashi, J. Normand, K. Raghavachari, A. Rendell, J. C. Burant, S. S. Iyengar, J. Tomasi, M. Cossi, N. Rega, J. M. Millam, M. Klene, J. E. Knox, J. B. Cross, V.

Bakken, C. Adamo, J. Jaramillo, R. Gomperts, R. E. Stratmann, O. Yazyev, A. J. Austin, R. Cammi, C. Pomelli, J. W. Ochterski, R. L. Martin, K. Morokuma, V. G. Zakrzewski, G. A. Voth, P. Salvador, J. J. Dannenberg, S. Dapprich, A. D. Daniels, O. Farkas, J. B. Foresman, J. V. Ortiz, J. Cioslowski, and D. J. Fox, , Gaussian 09, Revision A.02, Gaussian, Inc., Wallingford CT, 2009
17. C. Lee, W. Yang, and R. G. Parr, Development of the Colle Salvetti correlation-energy formula into a functional of the electron density, *Phys. Rev. B.*, 37 (1988) 785-789
18. P. Geerlings, F. D. Proft, and W. Langenaeker, Conceptual Density Functional Theory, *Chem. Rev.*, 103 (2003) 1793-1874
19. R. G. Parr and R. G. Pearson, Absolute hardness: Companion parameter to absolute electronegativity, *J. Am. Chem. Soc.*, 105 (1983) 7512-7516
20. R. G. Parr, L. V. Szentpaly, and S. Liu, Electrophilicity index, *J. Am. Chem. Soc.*, 121 (1999) 1922-1924
21. A. Kokalj and N. Kovacevic, On the consistent use of electrophilicity index and HSAB-based electron transfer and its associated change of energy parameters, *Chem. Phys. Lett.*, 507 (2011) 181-184
22. E. E. Ebenso, T. Arslan, F. Kandemirli, I. N. Caner, and I. I. Love, Quantum Chemical Studies of some Rhodamine Azosulpha Drugs as corrosion inhibitors for mild steel in Acidic Medium, *Int. J. Quantum Chem.*, 110 (2010) 1003-1018
23. P. Udhayakala and T. V. Rajendiran, A theoretical evaluation on benzothiazole derivatives as corrosion inhibitors on mild Steel, *Pharma Chem.*, 7 (2015) 92-99
24. V. Kouakou, P. M. Niamien, A. J. Yapo, and A. Trokourey, Copper Corrosion Inhibition in 1 M Nitric Acid: Adsorption and Inhibitive Action of Theophylline, *Chem. Sci. Rev. Lett.*, 5 (2016) 131-146
25. N. O. Eddy, S. R. Stoyanov, and E. E. Ebenso, Fluoroquinolones as Corrosion Inhibitors for Mild Steel in Acidic Medium, *Int. J. Electrochem. Sci.*, 5 (2010) 1127-1150
26. M. Yeo, P. M. Niamien, E. B. A. Bilé, and A. Trokourey, Thiamine Hydrochloride as a Potential Inhibitor for Aluminium Corrosion in 1.0M HCl: Mass Loss and DFT Studies, *J. Comput. Methods Mol. Des.*, 7 (2017) 13-25
27. C. Morell, A. Grand, and A. Torro-Labbé, Theoretical support for using the Δf (r) descriptor, *Chem. Phys. Lett.*, 425 (2006) 342-346
28. C. Morell, A. Grand, and A. Torro-Labbé, New Dual Descriptor for Chemical Reactivity, *J. Phys. Chem A.*, 109 (2005) 205-212
29. J. I. Martinez-Araya, Why is the dual descriptor a more accurate local reactivity descriptor than Fukui functions?, *J. Math. Chem.*, 53 (2015) 451-465
30. H. Keles, M. Keles, I. Dehri, and O. Serinday, Adsorption and inhibitive properties of aminobiphenyl and its Schiff base on mild steel corrosion in 0.5 M HCl medium, *Colloids Surf A: Physicochem Eng Aspects.*, 320 (2008) 138-145
31. M. R. Singh, K. Bhrara, and G. Singh, The Inhibitory Effect of Diethanolamine on Corrosion of Mild Steel in 0.5 M Sulphuric Acidic Medium, *Port Electrochim Acta.* 26 (2008) 479-492
32. S. Issadi, T. Douadi, A. Zouaoui, S. Chafaa, M. A. Khan, and G. Bouet, Novel Thiophene symmetrical Schiff base compounds as corrosion inhibitor for mild steel in acidic media, *Corros. Sci.*, 53 (2011) 1484-1488
33. X. Li, S. Deng, H. Fu, and G. Mu, Synergistic inhibition effect of rare earth cerium (IV) ion and anionic surfactant on the corrosion of cold rolled steel in H2SO4 solution, *Corros. Sci.*, 50 (2008) 2635- 2645
34. S. A. Umoren, Inhibition of aluminium and mild steel corrosion in acidic medium using gum Arabic, *Cellulose.*, 15 (2008) 751-761
35. N. Chaubey, Savita, V. K. Singh, and M. A. Quraishi, Corrosion inhibition performance of different bark extracts on aluminium in alkaline solution, *J. Assoc. Arab Univ. Basic Appl. Sci.*, 22 (2017) 38-44
36. L. Afia, R. Salghi, A. Zarrouk, H. Zarrok, O. Benali, B. Hammouti, *et al.*, Inhibitive action of argan press cake extract on the corrosion of steel in acidic media, *Port. Electrochim. Acta.*, 30 (2012) 267-279
37. N. Y. S. Diki, G. G. D. Diomandé, S. J. Akpa, A. Ouédraogo, L. A. G. Pohan, P. M. Niamien, and A. Trokourey, Aluminum Corrosion Inhibition by 7-(Ethylthiobenzimidazolyl) Theophylline in 1M Hydrochloric Acid: Experimental and DFT Studies, *Int. J. Appl. Pharm. Sci. Res.*, 3 (2018) 41-53
38. G. Gece and S. Bilgic, Quantum chemical study of some cyclic nitrogen compounds as corrosion inhibitors of steel in NaCl media, *Corros. Sci.*, 51 (2009) 1876-1878
39. I. A. Adejoro, C. U. Ibeji, and D. C. Akintayo, Quantum Descriptors and Corrosion Inhibition Potentials of Amodaquine and Nivaquine, *Chem. Sci. J.*, 8 (2017) 149-154
40. I. B. Obot, N. O. Obi-Egbedi, and S. A. Umoren, Adsorption Characteristics and Corrosion Inhibitive Properties of Clotrimazole for Aluminium Corrosion in Hydrochloric Acid, *Int. J. Electrochem. Sci.*, 4 (2009) 863 - 877
41. N. Khalil, Quantum chemical approach of corrosion inhibition, *Electrochim. Acta.*, 48 (2003) 2635-2640

42. K. F. Khaled, K. Babic-Samardziza, and N. Hackerman, Theoretical study of the structural effects of polymethylene amines on corrosion inhibition of iron in acid solutions, *Electrochim. Acta.*, 50 (2005) 2515-2520
43. G. Bereket, E. Hur, and C. Ogretir, Quantum chemical studies on some imidazole derivatives as corrosion inhibitors for iron in acidic medium, *J. Mol. Struct. :Theochem.*, 578 (2002) 79-88
44. G. Gece, The use of quantum chemical methods in corrosion inhibitor studies *Corros. Sci.*, 50 (2008) 2981-2992
45. G. Gece and S. Bilgic, Quantum chemical study of some cyclic nitrogen compounds as corrosion inhibitors of steel in NaCl media, *Corros Sci.*, 51 (2009) 1876-1878
46. P. Udhayakala, T. V. Rajendiran, and S. Gunasekaran, Theoretical approach to the corrosion inhibition efficiency of some pyrimidine derivatives using DFT method, *J. Comput. Methods Mol. Des.*, 2 (2012) 1-15
47. S. R. Stoyanov, S. Gusarov, M. S. Kuznicki, and A. Kovalenko, Theoretical Modeling of Zeolite Nanoparticle Surface Acidity for Heavy Oil Upgrading, *J. Phys. Chem. C.*, 112 (2008) 6794-6810

(2019) ; http://www.jmaterenvironsci.com